

# Low-temperature thermoelectric properties of bilayer graphene

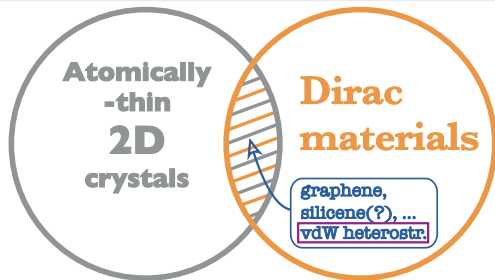
Adam Rycerz, Dominik Suszalski, and Grzegorz Rut  
*Marian Smoluchowski Institute of Physics, Jagiellonian University,  
Kraków, Poland*



StoCP 2018, Zakopane, Poland, September 16–21, 2018



# Why graphene?



- h-BN, h-AlN(?)
- MoS<sub>2</sub>, HfSe<sub>2</sub>, ...
- Black-P
- TiSe<sub>2</sub> (CWD+SC!)
- Artificial graphenes & analogs
- Topolog. insulators: HgTe/CdTe, Bi<sub>1-x</sub>Sb<sub>x</sub>, Bi<sub>2</sub>Se<sub>3</sub>, Bi<sub>2</sub>Te<sub>3</sub>, ...
- *d*-wave superconductors
- Weyl semimetals

For a review of the topic, see: [Wehling et al., Adv. Phys. 76, 1 \(2014\)](#).

Theory of SC in TiSe<sub>2</sub>: [Chen et al., arXiv:1806.08064](#).

# Emergent Dirac fermions in graphene

4 August 1972, Volume 177, Number 4047



## SCIENCE

### More Is Different

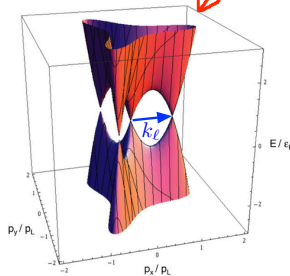
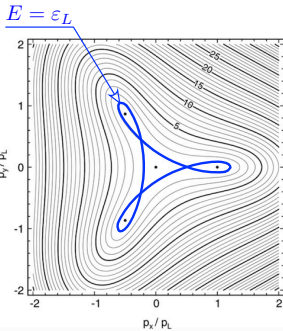
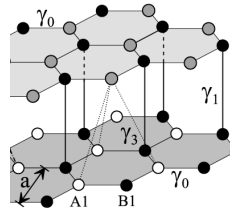
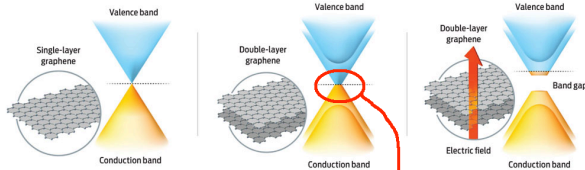
Broken symmetry and the nature of  
the hierarchical structure of science.

P. W. Anderson

## What differs graphene from a collection of carbon atoms?

- The **valley pseudospin** (  $\Rightarrow$  *fermion doubling* )
- Time-reversal symmetry breaking at zero magnetic field
- Pseudodiffusive charge transport, . . . , **SC in twisted-BLG** (!)

# Tunable band gap and trigonal warping



$$\epsilon_L = \frac{\gamma_1}{4} \left( \frac{\gamma_3}{\gamma_0} \right)^2 \approx 1 \text{ meV}$$

$$k_l = \frac{2}{\sqrt{3}} \frac{\gamma_1 \gamma_3}{a \gamma_0^2} \approx 0.05 \text{ nm}^{-1}$$

**Figure 4.** (a) Trigonal warping of the equi-energy lines in the vicinity of each  $K$  point, and the Lifshitz transition in bilayer graphene. The energy is in units of  $\epsilon_L$ . (b) Corresponding three-dimensional plot of the low-energy dispersion.

[ Top: IEEE Spectrum, 2009; bottom: McCann & Koshino, 2013 ]

**Table 1.** Values (in eV) of the SWM model parameters [64–67] determined experimentally. Numbers in parentheses indicate estimated accuracy of the final digit(s). The energy difference between dimer and non-dimer sites in the bilayer is  $\Delta' = \Delta - \gamma_2 + \gamma_3$ . Note that next-nearest layer parameters  $\gamma_2$  and  $\gamma_3$  are not present in bilayer graphene.

Parameter	Graphite [67]	Bilayer [76]	Bilayer [55]	Bilayer [56]	Bilayer [80]	Trilayer [82]
$\gamma_0$	3.16(5)	2.9	3.0 <sup>a</sup>	—	3.16(3)	3.1 <sup>a</sup>
$\gamma_1$	0.39(1)	0.30	0.40(1)	0.404(10)	0.381(3)	0.39 <sup>a</sup>
$\gamma_2$	-0.020(2)	—	—	—	—	-0.028(4)
$\gamma_3$	0.315(15)	0.10	0.3 <sup>a</sup>	—	0.38(6)	0.315 <sup>a</sup>
$\gamma_4$	0.044(24)	0.12	0.15(4)	—	0.14(3)	0.041(10)
$\gamma_5$	0.038(5)	—	—	—	—	0.05(2)
$\Delta$	-0.008(2)	—	0.018(3)	0.018(2)	0.022(3)	-0.03(2)
$\Delta'$	0.050(6)	—	0.018(3)	0.018(2)	0.022(3)	0.046(10)

<sup>a</sup> This parameter was not determined by the given experiment, the value quoted was taken from previous literature.

- [55] Zhang *et al.*, Phys. Rev. B **78**, 235408 (2008).  
 [56] Li *et al.*, Phys. Rev. Lett. **102**, 037403 (2009).  
 [67] Dresselhaus & Dresselhaus, Adv. Phys. **51**, 1 (2002).  
 [76] Malard *et al.*, Phys. Rev. B **76**, 201401(R) (2007).  
 [80] Kuzmenko *et al.*, Phys. Rev. B **80**, 165406 (2009).  
 [82] Taychatanapat *et al.*, Nature Phys. **7**, 621 (2011).

$$\varepsilon_L = \frac{\gamma_1}{4} \left( \frac{v_3}{v} \right)^2 \approx 1 \text{ meV}$$

Yankowitz *et al.*, (2014):  $\gamma_1 = 0.39 \text{ eV}$ ,  $\gamma_4 = 0.22 \text{ eV}$ , but  $\gamma_3$  not determined ...

⇒ **Novel phenomena governed solely by  $\gamma_3$  desired!**

## Where to expect TW effects on transport?

Time-energy uncertainty relation **limits the energy resolution:**

$$\Delta E \geq \frac{\hbar}{\Delta t} \sim \frac{\hbar v_F}{L},$$

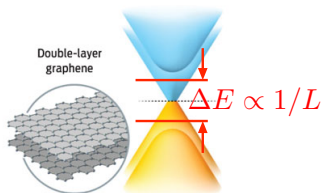
where we set  $\Delta t \sim t_{\text{flight}} \approx L/v_F$ .

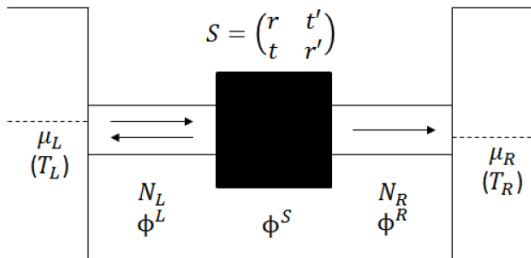
The condition  $\Delta E \lesssim 2\varepsilon_L$  leads to

$$L \gtrsim \frac{\hbar v_F}{2\varepsilon_L} = \sqrt{3} \frac{\gamma_0^3}{\gamma_1 \gamma_3^2} a \approx 400 \text{ nm},$$

where  $\gamma_0 = 3.16 \text{ eV}$ ,  $\gamma_1 = 0.38 \text{ eV}$ ,  $\gamma_3 = 0.3 \text{ eV}$ ,  $a = 0.246 \text{ nm}$ .

**⇒ Effects of  $\gamma_3 \neq 0$  on transport prop-s may depend on the system size; the crossover range:  $100 \text{ nm} < L < 1 \mu\text{m}$ .**





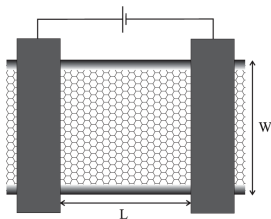
## Electric and thermal currents

$$I = -\frac{g_s g_v e}{h} \int dE T(E) [f_L(E) - f_R(E)],$$

$$I_Q = \frac{g_s g_v}{h} \int dE T(E) [f_L(E) - f_R(E)] (E - \mu),$$

where  $g_s = g_v = 2$  denote spin and valley degeneracies,  $T(E) \equiv \text{Tr}(\mathbf{t}\mathbf{t}^\dagger)$ , and  $f_L, f_R$  are Fermi-Dirac distributions.

# Monolayer at the charge-neutrality point



$$G = \frac{2e^2}{h} \sum_{n=-\infty}^{\infty} \frac{1}{\cosh^2[\pi(n + \alpha)L/W]}$$

$$\underset{\approx}{\underset{w \gg L}{\approx}} \frac{4e^2}{\pi h} \frac{W}{L},$$

where  $\alpha = \frac{1}{2}$  for the *mass confinement* ( $\Psi_A|_{y=0} = \Psi_B|_{y=0}$ ,  $\Psi_A|_{y=W} = -\Psi_B|_{y=W}$ ).

**The conductivity:**  $\sigma = GL/W = 4e^2/(\pi h) \equiv \sigma_0$ .

**Theory:** Katsnelson (2006); Tworzydło et al. (2006)

**Experiment:** Miao et al., (2007); Danneau et al., (2008).



# Emergent conductivity of BLG

- Landauer conductivity [Snyman & Beenakker, 2007],  $\underline{\gamma_3 = \gamma_4 = 0}$ :

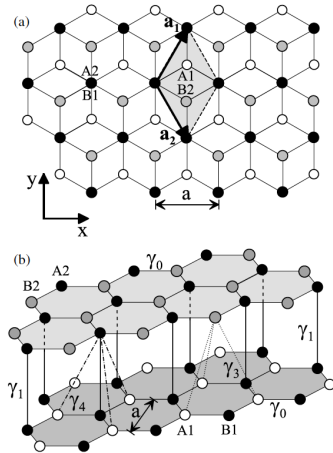
$$\sigma_{\text{bilayer}} = GL/W = 2\sigma_0$$

- Kubo conductivity [Cserti et al., 2007],  $\underline{\gamma_3 \neq 0}$ :

$$\sigma_{\text{bilayer}} = 6\sigma_0 (!)$$

- Experiment:** [Mayorov et al., 2011]  $\sigma_{\text{bilayer}} \simeq 5\sigma_0$ .

[ with  $\sigma_0 \equiv (4/\pi)e^2/h$  – **universal conductivity of a monolayer.** ]



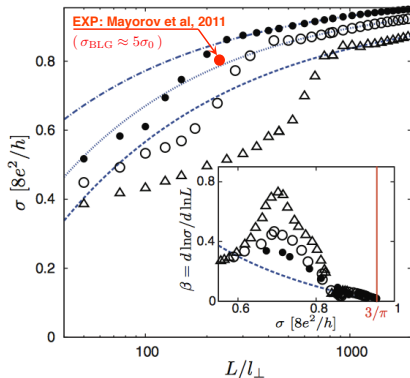


Fig. 3: (Colour on-line) Minimal conductivity of an unbiased graphene bilayer as a function of the sample length  $L$  (specified in units of  $l_{\perp} = \hbar v_F / t_{\perp} \simeq 1.60$  nm). Different datapoints correspond to different values of the next-nearest neighbor interlayer hopping:  $t' = 0.1$  eV ( $\Delta$ ),  $0.2$  eV ( $\circ$ ), and  $0.3$  eV ( $\bullet$ ).

[ Notation:  $t_{\perp} \equiv \gamma_1$ ,  $t' \equiv \gamma_3$  ]

## Non-commuting limits:

$$\lim_{L \rightarrow \infty} \lim_{d \rightarrow \infty} \sigma_{\text{BLG}} = 2\sigma_0$$

$$\lim_{d \rightarrow \infty} \lim_{L \rightarrow \infty} \sigma_{\text{BLG}} = 6\sigma_0 (!)$$

[  $\gamma_1 \sim \gamma_3 \sim e^{-Bd/d_0}$ ,  $\epsilon_L \sim \left( e^{-Bd/d_0} \right)^3$ ,  
and thus  $\epsilon_L / \gamma_1 \rightarrow 0$  with  $d \rightarrow \infty$   
(the interlayer distance) ]

**Surprising analogy with systems showing spontaneous symmetry breaking !**

Grzegorz Rut & AR:

$\Rightarrow$  PRB **89**, 045421 (2014)

$\Rightarrow$  EPL **107**, 47005 (2014)

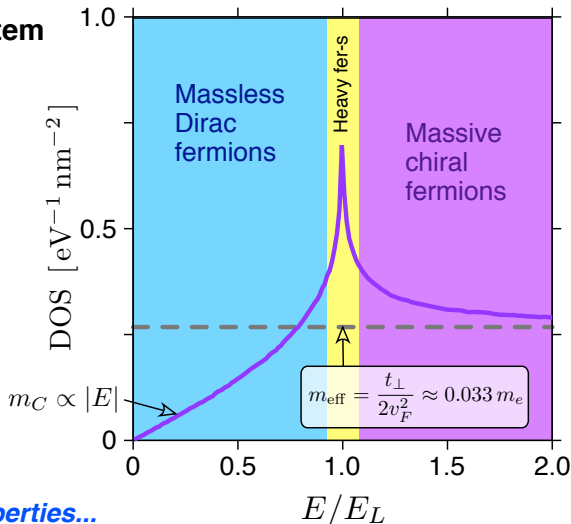
# Quasiparticles in *doped* BLG

In a generic 2D system

the cyclotron mass:

$$m_C(E) = \frac{\pi \hbar^2}{2} \text{DOS}(E)$$

Transitions between different populations of quasiparticles should have signatures in thermoelectric properties...



# Why thermoelectrics?

**The Mott formula** for metals [Cutler & Mott, Phys. Rev. (1969)]

$$S \approx \frac{\pi^2 k_B^2 T}{3e} \left[ \frac{\partial \ln \sigma(E)}{\partial E} \right]_{E=E_F},$$

**The Drude conductivity:**  $\sigma = ne^2\tau/m_{\text{eff}} \sim \text{DOS}(E_F) \times k_B T$   
(provided that the mobility  $\tilde{\mu}(E) \sim \tau/m_{\text{eff}} \approx \text{const.}$ ).

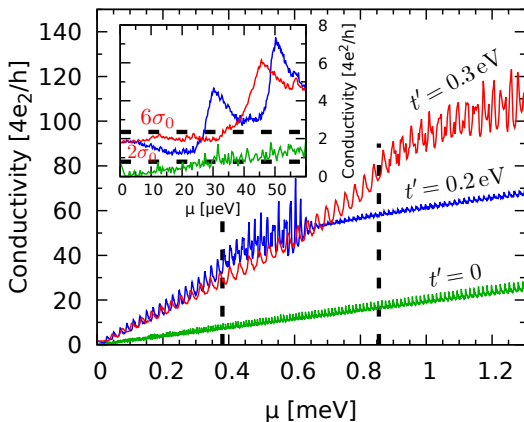
$\Rightarrow$  **Any abrupt change in DOS(E) should have some signature in S.**

**The Goldsmid-Sharp energy gap** in semiconductors

$|S|_{\text{max}} \approx E_g/(2eT_{\text{max}})$  allows the thermoelectric-based  
band-gap ( $E_g$ ) determination, instead of employing the familiar  
activation formula  $\sigma \sim \exp(-E_g/2k_B T)$ .

[Goldsmid & Sharp, J. Electron. Mater. (1999)].

# Zero-temperature conductivity ( $\mu \neq 0$ )



**Fabry-Perrot resonances:**  $\Delta E \approx 2\pi(\hbar v_F/L)\sqrt{|E|/t_\perp}$  for  $t' = 0$ , or  
 $\Delta E \sim \pi\hbar v_3/L = 2\pi(\hbar v_F/L)\sqrt{E_L/t_\perp}$  for  $t' \neq 0$ .

Above:  $L = 10^4 l_\perp = 17.7 \mu\text{m}$ . [[Suszalski, Rut, AR, PRB \(2018\)](#)]

In the linear-response regime:

$$G = \frac{I}{V} \Big|_{\Delta T=0} = e^2 L_0,$$

$$S = - \frac{V}{\Delta T} \Big|_{I=0} = \frac{L_1}{e T L_0},$$

$$K_{\text{el}} = \frac{I_Q}{\Delta T} \Big|_{I=0} = \frac{L_0 L_2 - L_1^2}{T L_0},$$

with  $L_n$  given by

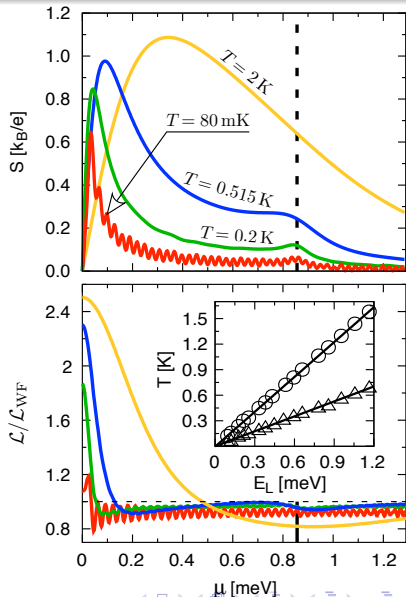
$$L_n = \frac{g_s g_v}{h} \int dE T(E) \left( -\frac{\partial f_{\text{FD}}}{\partial E} \right) (E - \mu)^n$$

The Lorentz number

$$\mathcal{L} = \frac{K_{\text{el}}}{T G} = \frac{L_0 L_2 - L_1^2}{e^2 T^2 L_0^2}$$

[  $\mathcal{L}_{\text{WF}} \equiv \frac{1}{3} \pi^2 (k_B/e)^2 \Leftrightarrow T(E) = \text{const}$ ;  
a model  $T(E) \propto |E| \Leftrightarrow \mathcal{L}_{\text{max}} \approx 2.37 \mathcal{L}_{\text{WF}}$ . ]

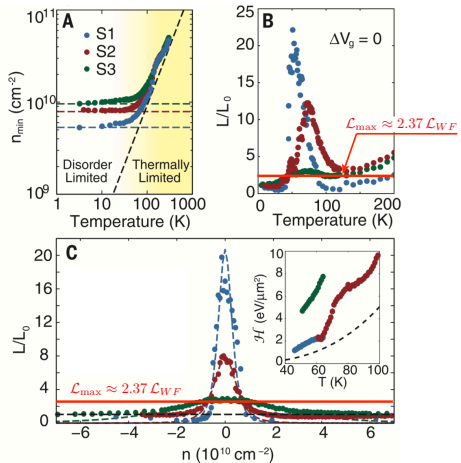
[ *Suszalski, Rut, AR, PRB (2018)* ]



⇒ **One does not necessarily need to include interactions to understand some experimental data!**

**Fig. 3. Disorder in the DF. (A)**

Minimum carrier density as a function of temperature for all three samples. At low temperatures, each sample is limited by disorder. At high temperatures, all samples become limited by thermal excitations. Dashed lines are a guide for the eye. **(B)** Lorentz ratio of all three samples as a function of bath temperature. The largest WF violation is seen in the cleanest sample. **(C)** The gate dependence of the Lorentz ratio is well fit to the hydrodynamic theory of (5, 6). Fits of all three samples are shown at 60 K. All samples return to the FL value (black dashed line) at high density. The inset graph shows the fitted enthalpy density as a function of temperature and the theoretical value in clean graphene (black dashed line). The schematic inset illustrates the difference between heat and charge current in the neutral Dirac plasma.



[ **EXP:** Crossno et al, Science (2016) ]

Chemical potential  $\mu$  is not a directly-measurable quantity, but it is **monotonically-dependent on the carrier density  $n$** .

**Characteristic temperatures**, at which the secondary maximum of  $S$  (minimum of  $\mathcal{L}$ ) vanishes are:

$$T_{\star}^S = 0.050 \times E_L/k_B,$$

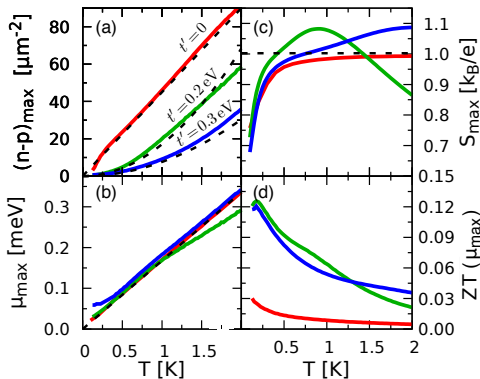
$$T_{\star}^{\mathcal{L}} = 0.118 \times E_L/k_B.$$

(For  $t' = 0.3$  eV,  $E_L/k_B \approx 10$  K.)

Also, a **global maximum of  $S$**  corresponds to

$$T_{\max}^S = 0.20 \times E_L/k_B.$$

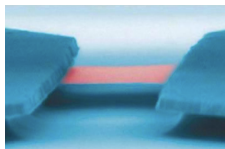
[ [Suszalski, Rut, AR, PRB \(2018\)](#) ]





# Remarks on *intrinsic* gap in BLG (1)

## Free-standing (suspended) BLG:



[Credit: Lau lab, UC Riverside]

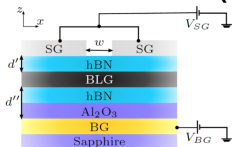
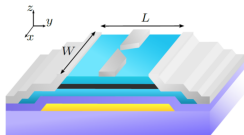
Width of resistivity peak matches the self-consistent (*mean-field*) gap:

$$\Delta_i(T) = \Delta_i(0) \tanh \left( 1.74 \sqrt{\frac{T_c}{T} - 1} \right) \text{ for } T \leq T_c,$$

with  $\Delta_i(0) \approx 1.5 \text{ meV}$ ,  $T_c \approx 12 \text{ K}$  ( $\Delta_i(0)/k_B T_c \approx 1.5$ ).

[Nam et al., 2D Mater 2016; Morpurgo, Graph. Week 2018]

## BLG in v.d. Walls heterostructures (vdWH):



**No signatures of  $\Delta_i > 0$  found as yet (!)**

[Kraft et al., Nat. Comm 2018]

## Remarks on *intrinsic* gap in BLG (2)

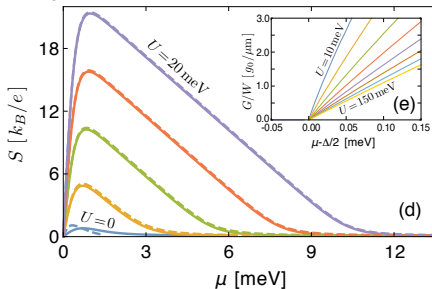
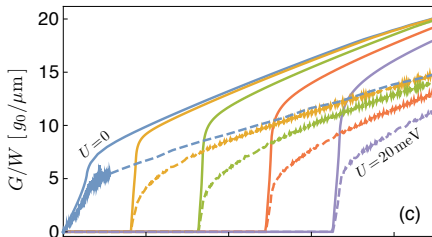
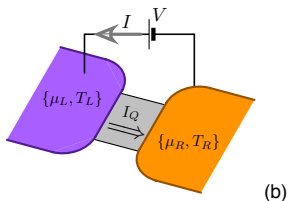
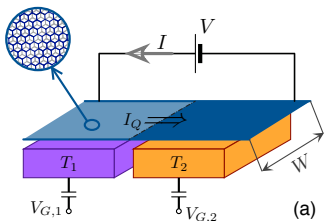
**Possible explanations** of the presence/absence of  $\Delta_i$  in free-standing BLG / vdWH containing BLG:

- Self-consistent gap strongly depends on effective Hubbard- $U$ :  $\Delta_i \sim t_0 \exp(-const/U_{\text{eff}})$  [Hirsch, 1985].

**Suppression of  $U_{\text{eff}}$  due to dielectric constant may dramatically reduce  $\Delta_i$  and  $T_C$ .**

- Lattice mismatch between BLG and h-BN induces an effective potential (*Moiré pattern*) destabilizing *quasi*-long range order (?)
- ...?

# The nonzero gap case ( $\Delta > 0$ )



[ Rut, Suszalski, AR, in preparation ]

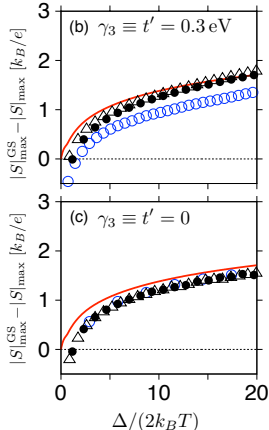
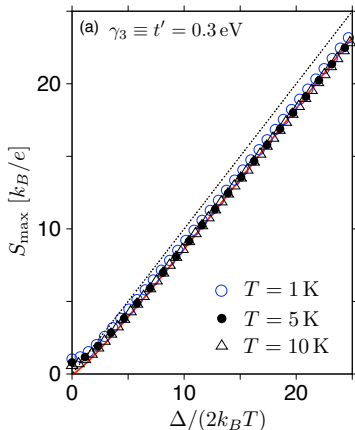
Dotted line:  
The reference  
(Goldsmid-Sharp)  
value:

$$|S|_{\max}^{\text{GS}} = \frac{\Delta}{2eT}$$

Red solid line:  
Approx/asymptotic  
expression [ $\Leftrightarrow T(E) \propto \Theta(|E| - \frac{1}{2}\Delta)$ ]

$$|S|_{\max} = |S|_{\max}^{\text{GS}} - (k_B/e) \times \left[ \frac{1}{2} \ln x + \ln 2 - \frac{1}{2} + \mathcal{O}(x^{-1}) \right], \text{ with } x = \Delta/2k_B T \gg 1.$$

[Rut, Suszalski, AR, in preparation]



# Thermoelectric figure of merit

$$ZT = \frac{\sigma S^2 T}{\kappa_{\text{el}} + \kappa_{\text{ph}}},$$

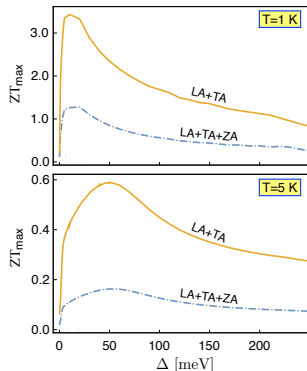
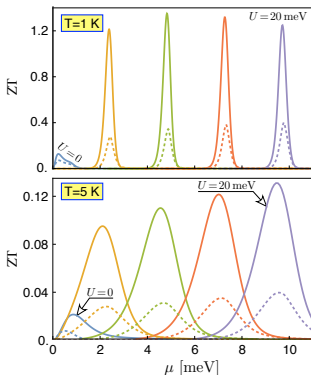
where  $\sigma$  is the electrical conductivity,  $S$ -the Seebeck coefficient,  $\kappa_{\text{el}}$  ( $\kappa_{\text{ph}}$ ) - electronic (phononic) part of the thermal conductivity.

In the linear-response regime, one can roughly approximate the maximal **energy conversion efficiency**

$$\eta = \frac{P_{\text{el}}}{I_Q} \approx \frac{1}{4} ZT \frac{\Delta T}{T} \left( = \frac{ZT}{4} \eta_{\star} \right)$$

(for  $\Delta T \ll T$ ), with  $P_{\text{el}}$  – the maximal (*usefull*) electric power and  $I_Q$  – the thermal current [see: Kim et al., PNAS **112**, 8205 (2015)].

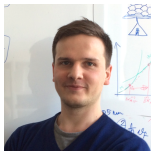
For instance,  $ZT=3$ ,  $\Delta T=100$  K and  $T=300$  K gives  $\eta \approx 0.25$ , comparable with  $\eta_{\star} = 0.33$  for a perfect Carnot engine.



$ZT = S^2 \sigma T / \kappa$ , with  $\kappa = \kappa_{\text{el}} + \kappa_{\text{ph}}$ . We have  $\mu_{\text{max}}^{ZT} \approx \Delta/2$ ; in contrast:  $\mu_{\text{max}}^S \approx \frac{1}{2} k_B T \ln(2\Delta/k_B T) \ll \Delta/2$ . In effect,  $ZT_{\text{max}}$  is sensitive to  $T(E)$  details near the band boundary and **does not grow monotonically with  $\Delta$**  (like  $|S|_{\text{max}}$ ). Instead, **ZT reaches a global maximum for  $\Delta_{\text{max}} \sim 10^2 k_B T$** . [*Rut, Suszalski, AR, in preparation*]

# Acknowledgments

## The group:



Grzegorz Rut Dominik Suszalski

**Former collaboration:** Anton Akhmerov, Jens Bardarson, Carlo Beenakker, Patrik Recher, Klaus Richter, Björn Trauzettel, Jakub Tworzydło, Michael Wimmer, ...

**Funding:**  NATIONAL SCIENCE CENTRE  
POLAND



Foundation for Polish Science



**Project web site:** <http://th.if.uj.edu.pl/~adamr/sonata.html>

**See also:** Suszalski et al., **POSTER NO. 15**

Rut et al., **POSTER NO. 13**

# THANK YOU!